agriculture

MDPI

Article

Determining Threshold Values for a Crop Water Stress Index-Based Center Pivot Irrigation with Optimum Grain Yield

Anzhen Qin, Dongfeng Ning *, Zhandong Liu *, Sen Li, Ben Zhao and Aiwang Duan

Key Laboratory of Crop Water Use and Regulation, Ministry of Agriculture and Rural Affairs, Institute of Farmland Irrigation, Chinese Academy of Agricultural Sciences, Xinxiang 453002, China; qinanzhen@caas.cn (A.Q.); lisen18@caas.cn (S.L.); zhaoben@caas.cn (B.Z.); duanaiwang@caas.cn (A.D.)
* Correspondence: ningdongfeng@caas.cn (D.N.); liuzhandong@caas.cn (Z.L.); Tel.: +86-373-3393321 (Z.L.)

Abstract: The temperature-based crop water stress index (CWSI) can accurately reflect the extent of crop water deficit. As an ideal carrier of onboard thermometers to monitor canopy temperature (T_c), center pivot irrigation systems (CPIS) have been widely used in precision irrigation. However, the determination of reliable CWSI thresholds for initiating the CPIS is still a challenge for a winter wheat–summer maize cropping system in the North China Plain (NCP). To address this problem, field experiments were carried out to investigate the effects of CWSI thresholds on grain yield (GY) and water use efficiency (WUE) of winter wheat and summer maize in the NCP. The results show that positive linear functions were fitted to the relationships between CWSI and canopy minus air temperature ($T_c - T_a$) ($r^2 > 0.695$), and between crop evapotranspiration (ET_c) and T_c ($r^2 > 0.548$) for both crops. To make analysis comparable, GY and WUE data were normalized to a range of 0.0 to 1.0, corresponding the range of CWSI. With the increase in CWSI, a positive linear relationship was observed for WUE ($r^2 = 0.873$), while a significant inverse relationship was found for the GY ($r^2 = 0.915$) of winter wheat. Quadratic functions were fitted for both the GY ($r^2 = 0.856$) and WUE ($r^2 = 0.629$) of summer maize. By solving the cross values of the two GY and WUE functions for each crop, CWSI thresholds were proposed as being 0.322 for winter wheat, and 0.299 for summer maize, corresponding to a $T_c - T_a$ threshold value of 0.925 and 0.498 °C, respectively. We conclude that farmers can achieve the dual goals of high GY and high WUE using the optimal thresholds proposed for a winter wheat–summer maize cropping system in the NCP.

Keywords: canopy temperature; soil water storage; crop evapotranspiration; infrared thermometer; *Triticum aestivum* L.; *Zea mays* L.

Citation: Qin, A.; Ning, D.; Liu, Z.; Li, S.; Zhao, B.; Duan, A. Determining Threshold Values for a Crop Water Stress Index-Based Center Pivot Irrigation with Optimum Grain Yield. *Agriculture* **2021**, *11*, 958. https://doi.org/10.3390/agriculture11100958

Academic Editor: Pascual Romer

Received: 31 August 2021
Accepted: 30 September 2021
Published: 2 October 2021

1. Introduction

Irrigation plays a fundamental role in promoting agricultural production. With the development of irrigated farming, agriculture is the largest consumer of anthropic water on the planet, in which 70% of the global fresh water is consumed by the agricultural sector [1]. Precision irrigation is regarded as a promising technique to save water resources and promote agricultural sustainability [2]. In the North China Plain (NCP), sprinkler and drip irrigation methods are commonly used in precision irrigation. However, these techniques do not adapt well to a winter wheat (*Triticum aestivum* L.)–summer maize (*Zea mays* L.) cropping system due to the differences in row spacing, plant height, and planting densities between the crops [3]. A center pivot irrigation system (CPIS) is considered adaptable in the mechanized operation for both wheat and maize due to its adaptability to different crops [4]. In addition, due to the over-depletion of aquifers, the NCP has become the severest groundwater depression zone in the world [5]. This especially expedites the development of water-saving techniques, making precision irrigation an inevitable trend for future agriculture in this area.

Precise diagnosis of water stress is the basis of precision irrigation [6]. Up to now, most efforts have focused on soil water balance, or water potential-based approaches [7].

However, the low spatial resolution limits their practical use [8]. Compared with soil moisture measurement, remote sensing of canopy temperature (T_c) provides an alternative to previous methods [9]. Its basic principle is that stomata will close when crops suffer water stress, causing a significant increase in T_c [10]. Thus, T_c can be an indicator of crop water status [11]. Nowadays, rapid advances in infrared thermometers (IRTs) have made the measurement of T_c much easier than before [12,13]. In addition, IRTs provide a non-destructive and high-resolution solution compared with soil moisture monitoring [14,15]. They are practical to deploy aboard moving irrigation systems, including the CPIS [16]. However, T_c cannot be separately adopted to schedule irrigation unless combined with other meteorological parameters [17]. The most common T_c-based indices are the crop water stress index (CWSI) [18,19], and canopy minus air temperature difference ($T_c - T_a$) [20], but these indices are generally location-dependent, and are influenced by various factors, including irrigation techniques, crop species, and varieties [21,22].

Usually, drought stress intensifies with the increase in CWSI. A CWSI value of 0.0–0.3 means crops are well-watered, whereas a value of 0.3–0.6 means crops are subjected to water stress [23,24]. Practically, full irrigation can be difficult under the current background of water scarcity, while deficit irrigation can be an effective way to save water and achieve comparable or higher GY [25]. That means that the deficit CWSI threshold will be higher than the empirical values obtained with full irrigation. Generally, crop water stress can be diagnosed by measuring T_c, T_a and vapor pressure deficit (VPD). It has been reported that CWSI can accurately reflect the extent of crop water stress, and $T_c - T_a$ has a good relationship with CWSI [26]. Chen et al. (2005) believed that maintaining $T_c - T_a$ of winter wheat < 0.4 °C obtained the optimal grain yield, and CWSI of 0.4 is the key threshold to reflect the occurrence of water stress in winter wheat [27]. Meanwhile, a similar study argued that the $T_c - T_a$ threshold of winter wheat should be 1.3 °C, and that the average CWSI had a nonlinear relationship with GY, with an optimal CWSI range 0.18–0.23 for winter wheat [28]. Compared to a constant threshold value, Wei et al. (2014) proposed dynamic thresholds of $T_c - T_a$ at different growth stages, and argued that the range of $T_c - T_a$ at flowering, filling and maturity stages of winter wheat should be 0.4–0.6, 0.4–0.55 and 0.4–0.65 °C; the corresponding CWSI ranges were 0.26–0.47, 0.29–0.64 and 0.45–0.62, respectively [29]. Cui et al. (2005) investigated the different irrigation levels effects on maize yields, but failed to conclude on a reasonable CWSI threshold for summer maize due to adequate precipitation [30]. Similar results were also observed in the NCP in the published literature [31,32]. However, in the Great Plains of the USA, a CWSI value of 0.4 was reported to increase the WUE of spring maize from 2.3 to 2.5 kg m^{-3} with deficit irrigation [33], but in another study in North America, maize yields experienced a significant decrease at the CWSI limit of 0.4 [34]. Usually, the above-mentioned studies estimated CWSI limits under traditional sprinkler, drip, or flooding irrigation, while CPIS is known to cause different water use dynamics from the traditional techniques. Therefore, it is necessary to further explore the optimal CWSI thresholds for CPIS irrigated winter wheat and summer maize in the NCP.

We hypothesized that reliable CWSI thresholds for CPIS irrigated crops could be identified via the determinate relationships between CWSI and GY/WUE. The objectives of this study were to quantify the relationships among CWSI, $T_c - T_a$ and GY/WUE for winter wheat and summer maize in the NCP, and to identify reliable CWSI thresholds using a distinctly different methodology.

2. Materials and Methods

2.1. Site Description

Field experiments were carried out from October 2019 to September 2020 at the Xuchang Irrigation Experiment Station in the NCP (34°76′ N, 113°24′ E, a.s.l. 73 m) (Figure 1). The cropping system is a winter wheat–summer maize crop rotation. The study area has a continent temperate monsoon climate. The annual mean temperature is 14.7 °C, the annual mean precipitation is 698 mm and the annual sunshine is 2280 h. Mete-

orological data were obtained from a weather observatory near the experimental station, with monitored parameters including air temperature (T_a, °C), wind speed (U_2, m s^{-1}), solar radiation (Ra, MJ m^2 d^{-1}), relative humidity (RH, %), and precipitation (mm). The data were measured at the height of 2.0 m. During the growing season of 2019–2020, total precipitation was recorded as 769 mm, of which 26% fell in the winter wheat season, and the remaining 74% fell in the summer maize season. Reference evapotranspiration (ET_0) was 583 and 445 mm for winter wheat and summer maize, respectively (Figure 2). The soil is a *fluvo-aquic* soil [35]. The soil bulk density of the 0–60 cm soil layer was 1.35 g cm^{-3}, total nitrogen content was 1.28 g kg^{-1}, the total phosphorus content was 1.71 g kg^{-1}, and organic matter content was 20.3 g kg^{-1}, respectively. Detailed soil physical properties prior to the experiment were presented by Qin et al. (2019) [36].

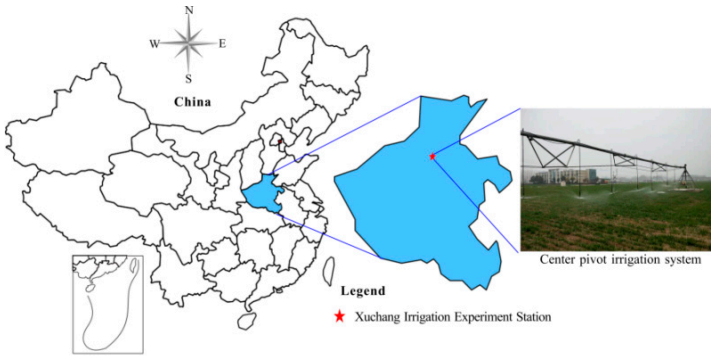

Figure 1. Schematic location of the Xuchang Irrigation Experiment Station.

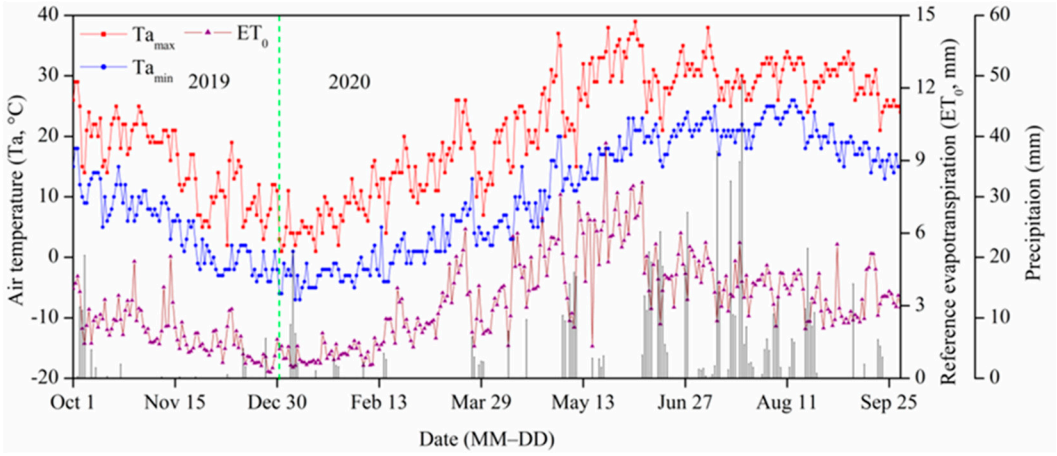

Figure 2. Maximum and minimum air temperature, reference evapotranspiration, and precipitation at the Xuchang Irrigation Experiment Station in the 2019–2020 growing season.

2.2. Experimental Design

Winter wheat seeds (*c.v.* Xinmai 26) were sown on 15 October, 2019, and were harvested on 29 May, 2020. The row spacing of wheat was 12 cm, and the basic number of seedlings was 2.25 × 10^6 plants ha^{-1}. A popular maize hybrid (*c.v.* Denghai 605) was selected in the experiment. Maize seeds were sown on 5 June 2020 and harvested on 30 September 2020. The plant spacing of maize was 30 cm, and the row spacing was 50 cm, giving a planting density of 6.75 × 10^4 plants ha^{-1}. Furrow dikes were installed in each inter-row following crop establishment to reduce surface movement of irrigation and precipitation water. Based on soil tests in the 0–100 cm soil profile, base fertilizers including urea (150 kg ha^{-1} N), diammonium phosphate (180 kg ha^{-1} P_2O_5), and potassium sulfate (55 kg ha^{-1} K_2O) were applied prior to sowing. To ensure a non-limited supply of nutrients for crops, additional urea (150 kg ha^{-1} N) was applied as a top dressing at the jointing

and flowering stages for both wheat and maize plants at a ratio of 6:4. All treatment plots received the same amounts of total fertilizer. Weeds and pests were managed according to the local governments' recommendations.

The CPIS consists of a pivot point, truss, overhang, lateral line, sprinkler and other components (Figure 3). The span (56.5 m) and overhang (3.5 m) are raised and supported on towers above the ground, allowing droppers connected to the lateral line, turning around the pivot point. The irrigated area is 1.13 ha. The flow rate per sprinkler is 0.2 to 0.6 LPS. The rate is controlled by a CPIS control-panel. Water pressure at the pivot point is 3.0 bar (43.5 psi). The spraying system optimizes the combination of sprinklers at different distances from the pivot point to ensure an irrigation uniformity of 90%. The height of the system is 3.0 m, and the height of droppers can be adjusted according to plant height. CPIS is a suitable platform that can transport infrared thermometers (IRTs) over cropped areas [37,38], on which IRTs are mounted to monitor spatial T_c data. When measuring T_c, rotational speeds can be managed to distribute the coverage of IRTs to all angular positions of the studied area [39]. A precision flow meter (Shanghai Water Meter Manufacturing Co. Ltd., Shanghai, China) was installed at the pump outlet to measure the irrigation volume.

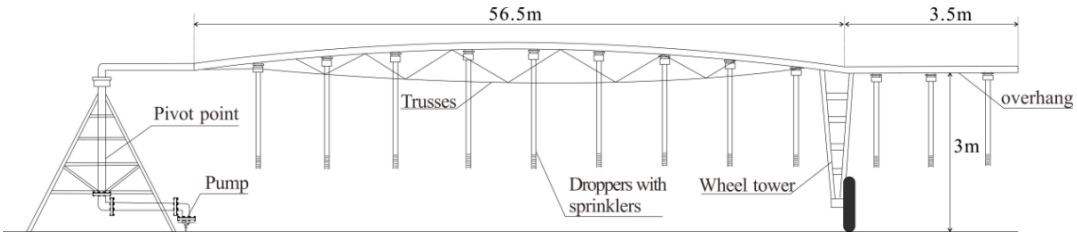

Figure 3. Main units and parameters of the center pivot irrigation system (CPIS).

After each crop sowing, all experimental plots were irrigated with 30 mm water to guarantee the uniform and rapid germination of seeds (Table 1). Otherwise, different irrigation levels were carried out during the growing season of wheat, whereas maize crops were mainly rain-fed. Every irrigation system has an E_a lower than 1, and gross irrigation must be larger than the net irrigation. In this study, net irrigation was also measured by rainfall gauges installed in each plot. Therefore, the irrigation amount calculated in the study was considered equal to net irrigation. Incomplete randomized block design was adopted with six replicates. Four irrigation treatments were set as follows: I1, supplying 45% of crop water requirements, I2, supplying 60%, I3, supplying 85% and I4, supplying 100% of crop water requirements, respectively. Three plots with the same treatments were in the same sector area, where: in zone I, the plot size was 353 m^2; in zone II, the plot size was 551 m^2; and in zone III, the plot size was 509 m^2 (Figure 4). Each experimental plot was surrounded by a border plot of the same size to avoid edge effects on the experimental plots. The inclusion of border plots effectively separated irrigation treatments. To induce slight drought and promote the penetration of roots of wheat, the irrigation quota was reduced at the over-winter and jointing stages, whereas more water was delivered at the critical flowering and filling stages [40,41]. The amount of full irrigation (I4) was calculated according to Equation (1), and detailed information of irrigation for different treatments was presented in Table 1. Averaged across the whole growing season, mean CWSI thresholds were 0.45, 0.35, 0.28, and 0.20 for I1, I2, I3, and I4 treatments. In Equation (1), field capacity was used as an indicator for the upper limit of water that can be used by plants, which was determined in the laboratory by measuring the amount of water retained at an applied pressure of −33 kPa, whereas wilting point was determined at an applied pressure of 1500 kPa [42]. In this study, the wilting point in the 0–30, 30–60, 60–100 cm soil depths was 11.4%, 12.3%, and 12.8% v/v, and the corresponding field capacity was 29.3%, 30.1%, and 32.8% v/v, respectively.

$$Q = 10 \times \sum_i (FC - SWC) \times D_i \quad (1)$$

where Q is the amount of full irrigation per single time (mm); FC is the field capacity (cm^3 cm^{-3}); SWC is the soil volumetric water content before irrigation (cm^3 cm^{-3}); and D_i is the planned wet layer depth (cm).

Table 1. Irrigation quota (mm) of different treatments for wheat and maize in the 2019–2020 growing season.

Treatments	Items	Wheat Season						Maize Season	
		Seedling	Over-Wintering	Jointing	Flowering	Filling	Total/Average	Seedling	Total
I1	Irrigation quota	30	15	16	32	25	118	30	30
	CWSI threshold	—	0.30	0.35	0.50	0.65	0.45	—	—
I2	Irrigation quota	30	21	27	46	42	166	30	30
	CWSI threshold	—	0.20	0.35	0.40	0.45	0.35	—	—
I3	Irrigation quota	30	37	46	64	55	232	30	30
	CWSI threshold	—	0.20	0.25	0.30	0.35	0.28	—	—
I4	Irrigation quota	30	50	53	75	66	274	30	30
	CWSI threshold	—	0.15	0.20	0.20	0.25	0.20	—	—
Planned wet layer depth (cm)		0–40	0–40	0–60	0–80	0–100	—	0–40	—

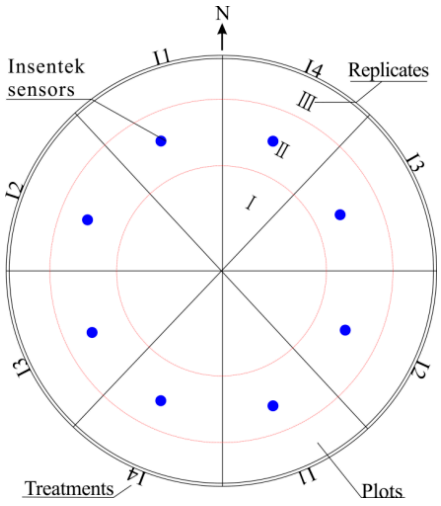

Figure 4. Plot layout of field experiment with the center pivot irrigation system (CPIS).

2.3. Data Collection and Measurements

2.3.1. Canopy Temperature

Infrared thermometers (IRTs) (Shi'ao Instrument Co. Ltd., Wuxi, China) with a band-pass of 5.5–14 µm were adopted to measure T_c. The measurement was implemented after the complete formation of wheat leaves on 15 November, 2019, and maize leaves on 20 June, 2020. Measurements were taken from 10:00 to 14:00 on a daily basis, when T_c typically reached diurnal maxima. The moving IRTs were aboard the CPIS. When measurement started, the CPIS rotated around the center pivot with an angular speed of 3° min^{-1}, and a wheel moving speed of 2.9 m min^{-1}. A round of data measurement took almost 2 h. Data were then divided and selected every 15 min per plot. Data were recorded every minute by the datalogger, and then were averaged and stored every 15 min. The IRTs had a field of view of 36°, a sensing window of 12.5 mm, and a resolution of 0.1 °C. The IRT array contained 9 thermometers that were positioned at regular intervals above the canopy. During each time period, 1080 measurements were taken, and a total of 270 T_c data were averaged to represent each treatment. The IRTs' view was periodically checked and adjusted. Data can be downloaded from the datalogger to a laptop computer via wireless data transmission.

2.3.2. Soil Water Content and Crop Evapotranspiration

Soil water content (SWC, % v/v) was measured at 10 cm increments to a depth of 100 cm using Insentek sensors (Zhejiang Oriental Insentek Technology Co. Ltd., Hangzhou, China). Sensors were installed in the central sector areas, and measured SWC every 10 min.

The average over two hours was stored in a data logger and was transmitted to a local server via wireless network. Our previous study indicated that the Insentek sensor was a reliable tool to represent real SWC values in the field with a root mean square error (RMSE) of 0.927% v/v between the Insentek sensor and oven-dry method (Table S1) [36]. Through checking the year-round data, data of Insentek sensors also had good continuity and stability [5]. Crops around the sensors were not missed and uniform, and were representative of the experimental conditions with the similar sizes and vigor.

Crop evapotranspiration (ET_c, mm) was calculated using soil water balance equation [25]:

$$ET_c = I + P - C_r - R_f - D_p \pm \Delta S \quad (2)$$

where ET_c is crop evapotranspiration (mm) during the growing season of wheat and maize, I is the amount of irrigation water applied (mm), P is the seasonal precipitation (mm) measured at the adjacent weather station, C_r is capillary rise (mm), R_f is runoff (mm), D_p is deep percolation (mm), and ΔS is the change in soil water storage (SWS, mm).

In Equation (2), C_r was considered to be zero, because the groundwater table was 5.0 m below the surface; R_f was also assumed to be zero because furrow dikes were used to control runoff; D_p was considered to be zero because SWC below 100 cm did not reach FC on the sampling dates.

2.3.3. Crop Water Stress Index

Daily CWSI was calculated as the average of 15 min CWSI values between 10:00 and 14:00 MST. The measurement time fell in the optimal measurement period proposed by the previous literature [32]. Although we cannot guarantee that every measurement was taken on a sunny and windless day, the data were averaged on a large number of measured values (270 data every time), which help to minimize the discrepancy in data and the adverse effect of weather factors. As an index indicating the severity of drought stress on plants, CWSI was adopted and defined as [43]:

$$CWSI = \frac{(T_c - T_a) - (T_c - T_a)ll}{(T_c - T_a) - (T_c - T_a)ul} \quad (3)$$

where $(T_c - T_a)ll$ is the lower limit of $T_c - T_a$, representing the non-water-stressed lower baseline, and $(T_c - T_a)ul$ is the upper limit of $T_c - T_a$, representing the non-transpiring upper baseline. In this study, $(T_c - T_a)ll$ from 100% supplying treatment was regarded as the lower non-stressed baseline. $(T_c - T_a)ul$ was estimated at 5 °C as the upper limit for most cereal crops [44,45].

2.3.4. Grain Yield and Water Use Efficiency

At physiological maturity, an area of 20 m^2 from 24 plots was harvested manually and grain mass was determined. Sampling plots were located at the same distance from a center pivot. The total numbers of plants and ears were counted, and the number of ears per plant was determined. Grain per ear was counted for each ear. Grain weight was determined by oven-drying three samples of 1000 kernels at 80 °C for 72 h to a constant weight. The grains were separated, cleaned, and weighed. Grain yield was expressed at 14% moisture content as determined using a PM–8188 portable moisture meter (Kett Electric Lab., Tokyo, Japan).

Water use efficiency (WUE, kg m^{-3}) was calculated as the grain yield (kg ha^{-1}) produced per unit of ET_c (mm).

$$WUE = \frac{GY}{ET_c} \times 0.1 \quad (4)$$

where GY is the grain yield (kg ha^{-1}) and ET_c is the crop evapotranspiration (mm) calculated according to Equation (2). The coefficient (0.1) converts kg ha^{-1} mm^{-1} to kg m^{-3}.

2.3.5. Determining Thresholds of CWSI and $T_c - T_a$

Data of GY and WUE were normalized to standardized values between 0.0 and 1.0 using min-max normalization [46], corresponding to the range of CWSI. The relationships between CWSI and normalized values of GY and between CWSI and normalized values of WUE were determined using Equation (5) for wheat and Equation (6) for maize. To achieve the dual goal of high GY and WUE, CWSI thresholds for initiating irrigation were determined using the cross values of the CWSI vs. GY functions and the CWSI vs. WUE functions:

$$NV_W = a \times CWSI + b \quad (5)$$

$$NV_M = a \times CWSI^2 + b \times CWSI + c \quad (6)$$

where NV_W and NV_M are the normalized values of GY or WUE for wheat and maize, respectively; *CWSI* is the crop water stress index; and *a*, *b*, and *c* are parameters fitted to the equations.

2.4. Statistical Analysis

Analysis of variance (ANOVA) was performed to test the differences in GY, WUE, T_c, and ET_c among treatments. Correlation analysis was conducted with SPSS 19.0 software (SPSS Institute Inc. USA) to determine the relationships between GY and CWSI, as well as the relationship between WUE and CWSI. Means were compared using Fisher's least significant difference tests at $p < 0.05$. Graphs presented were plotted using Sigmaplot 12.0 (Systat Software, San Jose, CA, USA).

3. Results and Discussion

3.1. Grain Yield and Water Use Efficiency

Less water supply induced more drought stress on crops, resulting in lower GY and WUE [47,48]. However, moderate drought during non–sensitive stages was shown to promote root penetration and improve WUE [49]. Through the optimization of irrigation water, deficit irrigation can be an effective way to attain comparable or higher GY while saving water [50]. For both wheat and maize under the I1–I3 treatments, GY and WUE significantly decreased with the increasing CWSI (Table 2). The I4 treatment with the best soil moisture conditions produced the highest GY of wheat. For maize, the I3 treatment produced the highest GY. However, the difference in GY between I3 and I4 was not significant for both crops. Compared to the I1 treatment, I2, I3 and I4 increased the GY of wheat by 9%, 15% and 20%, respectively. Low GY of wheat with I1 treatment was associated with significant water stress at critical stages [51]. Generally, increasing water supply increased ET_c, while decreasing WUE. For wheat, ET_c with the I2, I3 and I4 treatments was increased by 10%, 19% and 26%, respectively, compared to the I1 treatment, while for maize crops, ET_c was 6–15% higher with the I2–I4 treatments compared to the I1 treatment. The greatest WUE (1.58 kg m^{-3}) was observed with the I1 treatment for wheat, whereas for maize crops, I3 produced the highest WUE (2.32 kg m^{-3}). On the contrary, WUE with the I4 treatment was the lowest for both crops, implying that excessive water supply lowered WUE [52]. The study indicated that the responses of WUE to various drought levels differed among crop species. Wheat crops were more likely to generate high WUE under high CWSI (0.45), while maize plants generated the greatest WUE under moderate CWSI (0.28). Previous studies reported that mild water stress increased WUE, while high water stress imposed at critical stages decreased the WUE of wheat and maize markedly [28,30,34]. In this study, although precipitation in the maize growing season was adequate, supplemental irrigation of 30 mm was added after sowing. This was because initial SWC was well below the depletion threshold prior to maize sowing. On average, the initial SWC with I1 treatment was only 10.5% *v/v*, and that of I2–I4 treatments was 13.8% *v/v* in the 0–50 cm soil depth, which was very close to the wilt point (Figure S1). Low SWC was also observed during the vegetative period of maize, which finally caused yield losses of 6–10% with deficit irrigation treatments. The study implied that antecedent treatments

during the wheat season influenced the initial SWC of maize markedly, and thus caused significant ET_c and GY differences for maize crops under rain–fed conditions.

Table 2. Crop evapotranspiration, grain yield and water use efficiency of a winter wheat–summer maize cropping system with center pivot irrigation.

Treatments	CWSI Threshold	Irrigation Amount (mm)	SWS in 0–100 cm Soil Depth (mm)		ET_c (mm)	GY (kg ha^{-1})	WUE (kg m^{-3})
			Before Sowing	After Harvest			
Winter wheat							
I1	0.45	118	207	161	416 c	6585 c	1.58 a
I2	0.35	166	210	172	456 b	7155 b	1.57 a
I3	0.28	232	191	178	497 ab	7605 a	1.53 ab
I4	0.20	274	177	180	523 a	7892 a	1.51 b
Summer maize							
I1	0.45	30	141	271	467 c	10577 b	2.26 b
I2	0.35	30	174	276	495 b	11019 ab	2.23 b
I3	0.28	30	184	285	496 b	11523 a	2.32 a
I4	0.20	30	189	246	540 a	11276 a	2.09 c

Note: CWSI, crop water stress index; SWS, soil water storage; ET_c, crop evapotranspiration; GY, grain yield; WUE, water use efficiency. Different letters in the same column mean significant difference at $p < 0.05$.

3.2. Diurnal Dynamics of Canopy Temperature and Crop Evapotranspiration

Canopy temperature (T_c) can be used to predict water stress, since it was associated with soil water status [53]. For example, a significant decrease in T_c usually occurred after irrigation and precipitation (>10 mm) events (Figure 5A). The lowest T_c (–1.1 °C) occurred during the overwintering of wheat, whereas the highest T_c (40.4 °C) appeared at wheat maturity. On average, seasonal mean T_c with I1, I2, I3 and I4 was 23.5, 22.3, 21.9 and 21.2 °C, respectively. For maize crops, the lowest T_c (18.2 °C) appeared at the R6 stage, while the highest T_c (37.4 °C) appeared at the V12 stage. Previous studies pointed out that too low T_c might predict no stress [54,55]. The findings were also proven by our study in which CWSI was only 0.0–0.25 with significant low T_c in over-wintering, which might result in an incorrect irrigation decision [56]. Thus, T_c combined with soil moisture measurement may be a better way to quantify the water stress of wheat during the over-wintering period.

Diurnal dynamics of ET_c were stable from the sowing to seedling stages of wheat, with a mean value of 1.80 mm d^{-1} (Figure 5B). It gradually decreased to 0.09 mm d^{-1} during overwintering. ET_c increased with the increasing T_a during re-greening, and peaked in the middle period of the filling stage. The maximum ET_c of wheat was 5.95, 8.06, 8.36 and 8.45 mm d^{-1} for I1, I2, I3 and I4 treatments at mid-filling stage. From re-greening to maturity, the mean ET_c of I1, I2, I3 and I4 treatments was 3.48, 4.02, 4.25 and 4.71 mm d^{-1}, respectively. For maize, the highest ET_c was 7.71, 8.27, 8.41 and 8.45 mm d^{-1}, from the VT to R3 stages, respectively. The seasonal mean ET_c was 4.13, 4.38, 4.38 and 4.79 mm d^{-1} for summer maize.

3.3. Diurnal Dynamics of Crop Water Stress Index and $T_c - T_a$

Daily CWSI decreased after irrigation or precipitation events and increased during the period between events (Figure 6A). Generally, CWSI and $T_c - T_a$ had similar trends among treatments. CWSI dynamics varied inversely with irrigation levels, with an appropriate range of CWSI from 0.1 to 0.3. The result was consistent with the findings of previous studies conducted in China [28,29]. The lowest irrigation amount (I1) generated the highest CWSI of 0.63, which was 46%, 55% and 64% higher than those of I2, I3, and I4 treatments. Water stress significantly increased $T_c - T_a$ (Figure 6B). The minimum $T_c - T_a$ for wheat was −4.5 °C after over-wintering irrigation. It was found that $T_c - T_a$ values were basically negative the day after irrigation, which was consistent with the results of Chen et al. (2005) [27]. Several low $T_c - T_a$ values were also induced by heavy precipitation. The

maximum $T_c - T_a$ value (4.71 °C) was observed at the flowering stage of wheat with I1 treatment, which was 87%, 98% and 110% higher than that of I2, I3, and I4 treatments. The maximum $T_c - T_a$ value was very close to the upper $T_c - T_a$ limit of 5 °C proposed by Sepaskhah and Kashefipour (1994) [57]. During the maize season, only I1 treatment generated $T_c - T_a > 0$ °C, with a maximum value of 1.35 °C, and a CWSI of 0.37, at V12 stage.

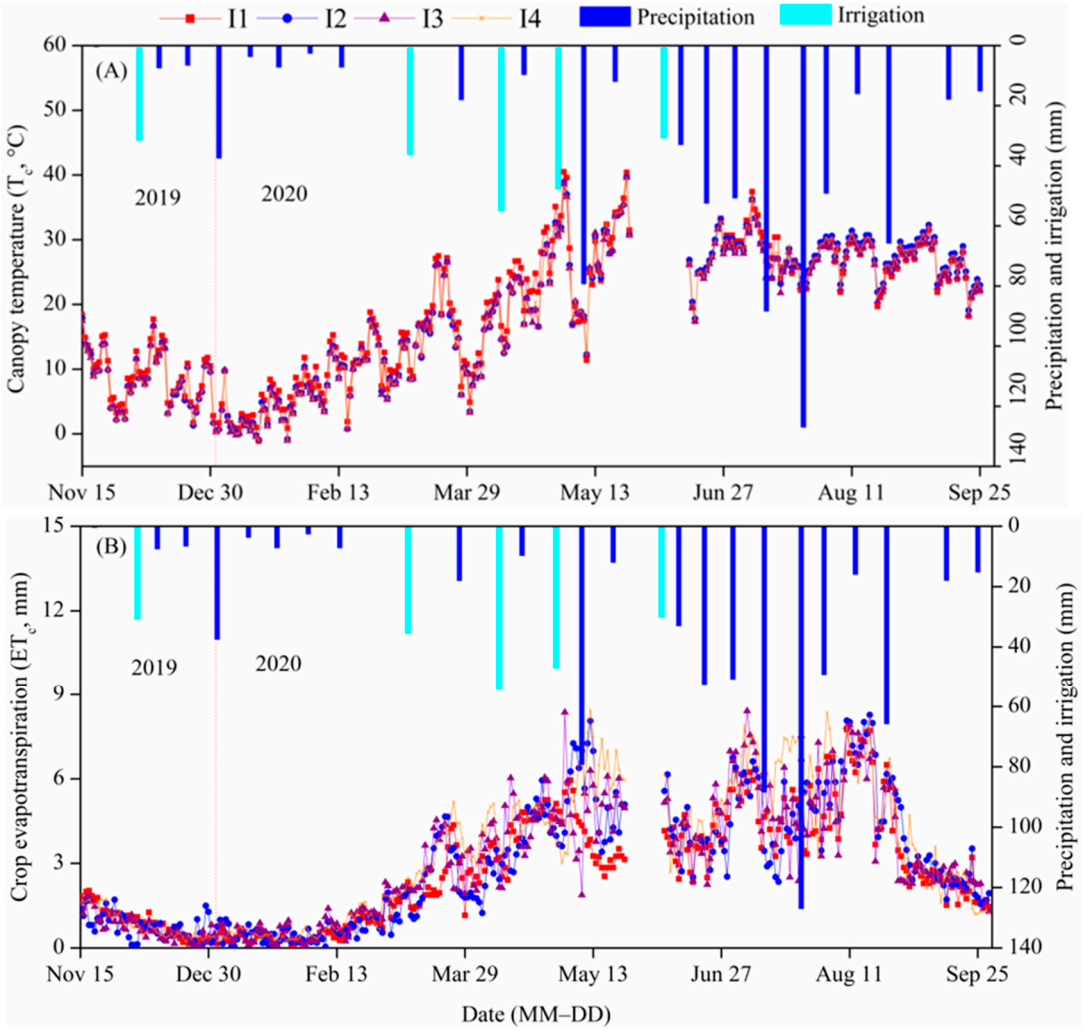

Figure 5. Seasonal variations in (**A**) canopy temperature (T_c, °C) and (**B**) crop evapotranspiration (ET_c, mm) in a winter wheat–summer maize cropping system in the 2019–2020 growing season. Precipitation is presented as ten-day cumulative values. Irrigation is average values among I1, I2, I3, and I4 treatments.

3.4. Correlation between ET_c and T_c and between CWSI and $T_c - T_a$

The relationship between CWSI and $T_c - T_a$ was fitted to a positive linear equation ($r^2 > 0.695$) (Figure 7A,C). The slopes for both wheat and maize crops were highest (0.055–0.059) with I1 treatment, implying that water stress accelerated the increasing rate of CWSI with $T_c - T_a$. As for I2–I4 treatments, they had similar slopes for both crops. A similar linear relationship between CWSI and $T_c - T_a$ was also observed in previous studies [58–60]. During the maize growing season, CWSI values fell in a proper range of relieved stress most of the time, which favored maize growth. Similarly, a significant linear relationship was observed between ET_c and T_c ($r^2 > 0.548$) (Figure 7B,D). The slopes increased with irrigation levels, indicating that the increasing rate of ET_c with T_c increased under well-watered conditions, whereas drought stress reduced the sensitivity of ET_c to

T_c for wheat and maize. Similar results were also observed in spring maize and alfalfa (*Medicago Sativa* Linn) under a semiarid climate in Northwest China [61].

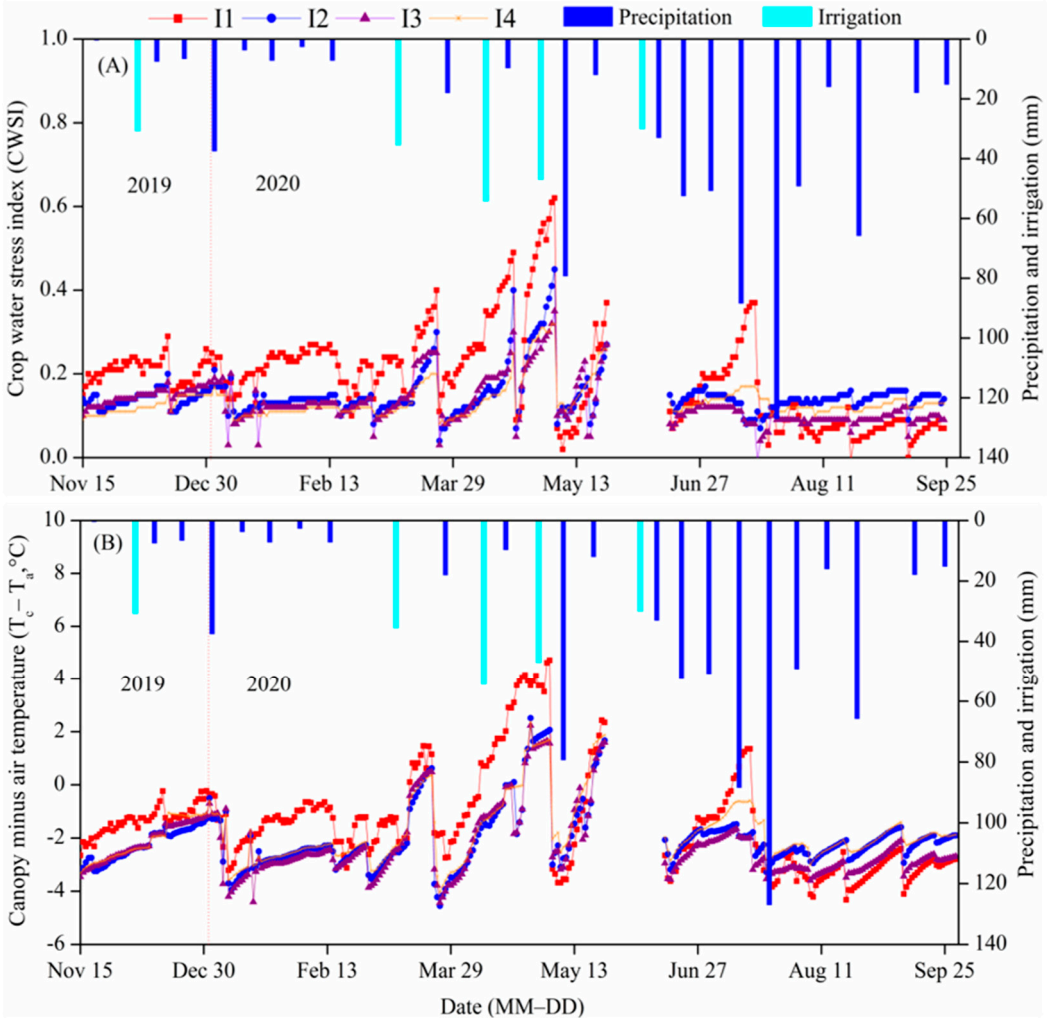

Figure 6. Dynamics of (**A**) crop water stress index (CWSI) and (**B**) canopy minus air temperature ($T_c - T_a$, °C) in a winter wheat–summer maize cropping system in 2019–2020 growing season. Precipitation is presented as ten-day cumulative values. Irrigation was average values among I1, I2, I3, and I4 treatments.

3.5. Determining the Thresholds of CWSI and $T_c - T_a$

Determining reliable CWSI thresholds is vital for precision irrigation, since it directly affects GY and WUE [48]. In order to make correlation analysis comparable, GY and WUE data were normalized to a range of 0.0 to 1.0. For wheat, linear decrease and increase relationships were observed for GY (r^2 = 0.915) and WUE (r^2 = 0.873) with increasing CWSI thresholds, respectively (Figure 8A). Meanwhile, for maize, quadratic equations were established for both GY (r^2 = 0.856) and WUE (r^2 = 0.629) (Figure 8B). The quadratic relationships between CWSI and GY were also reported in previous studies in terms of citrus (*Citrus reticulata Blanco*) and maize [62,63]. However, most studies reported a linear relationship between CWSI and GY in wheat, potato (*Solanum tuberosum* L.), and cotton (*Gossypium spp*) [27,64–67].

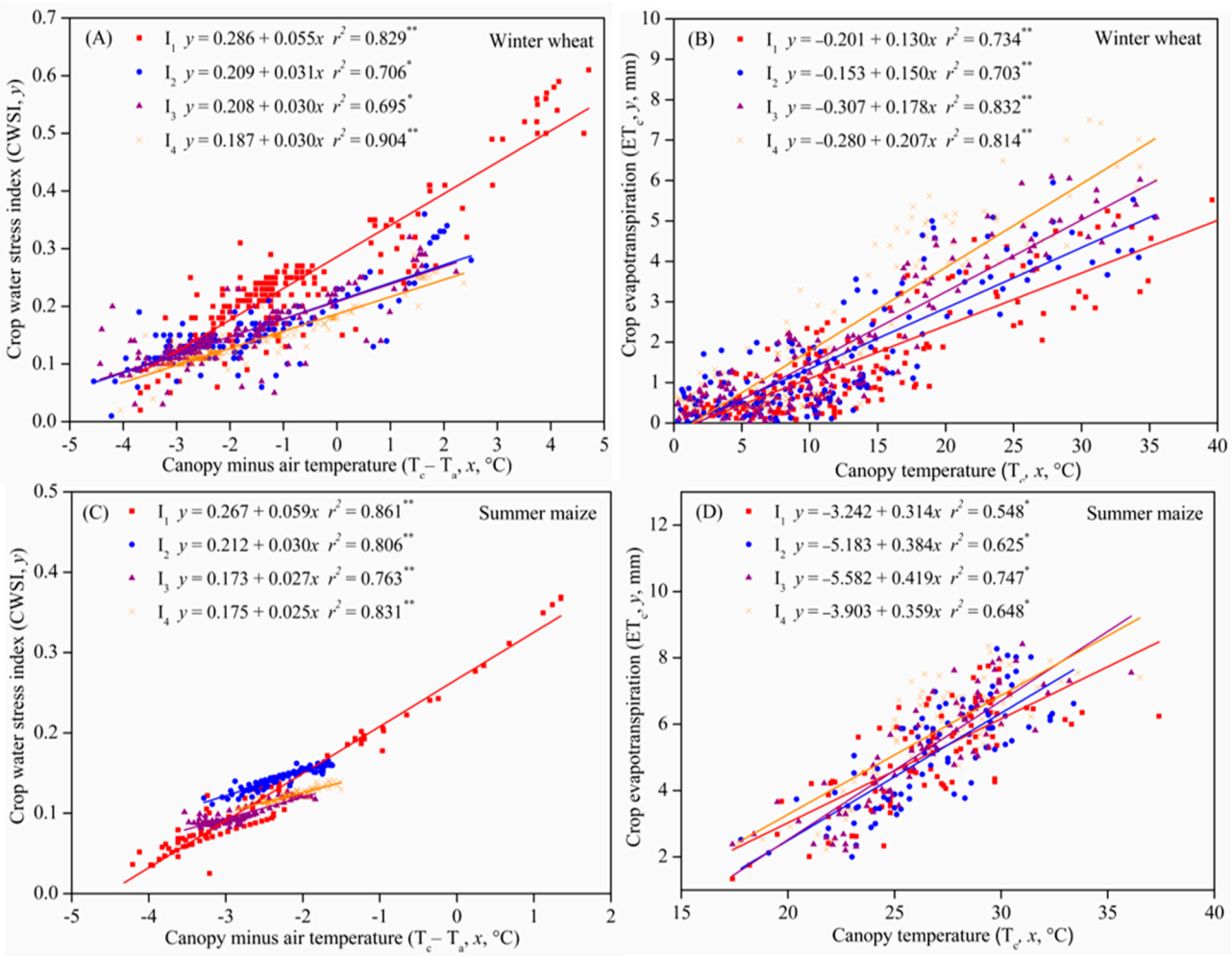

Figure 7. Positive linear equations fitted to the relationships (**A**,**C**) between crop water stress index (CWSI, y) and canopy minus air temperature ($T_c - T_a$, x), and (**B**,**D**) between crop evapotranspiration (ET_c, y) and canopy temperature (T_c, x) based on field experiments conducted in the 2019–2020 growing season. * and ** mean significant correlation at $p < 0.05$ and $p < 0.01$, respectively.

In the previous literature, the determination of CWSI thresholds was estimated mainly by experience, which was, to some extent, empirical [68–70]. Based on the functions proposed for wheat and maize crops, a distinctly different solution was adopted for the determination of reliable CWSI. In this study, the reliable threshold was defined as the one that can achieve the dual goal of high GY and high WUE. Based on the definition, we considered that the cross values of the two functions was the threshold value that satisfies the dual goal. For example, a normalized value of 0.575 was considered desirable at the CWSI threshold of 0.322 for winter wheat. The threshold value of wheat was very close to that estimated by Zhao (2016) in Hengshui in the NCP [68]. Similarly, an optimal threshold of 0.299 was expected for summer maize, since it obtained a high normalized value of 0.765. The threshold value of maize was higher than that estimated by Wang (2008), who conducted a similar experiment on summer maize in Wuhan, Central China, whose climate was more humid than Xuchang [69]. Compared with a sub-humid climate in this study, a CWSI limit of 0.22 was chosen for maize under the Mediterranean semiarid climate [44], implying that climatic conditions had noticeable effects on CWSI thresholds. In the sub-humid subtropical region of India, it was reported that the threshold of CWSI should be maintained below 0.30 for the optimum yield of wheat [70], which was very close to the threshold in this study.

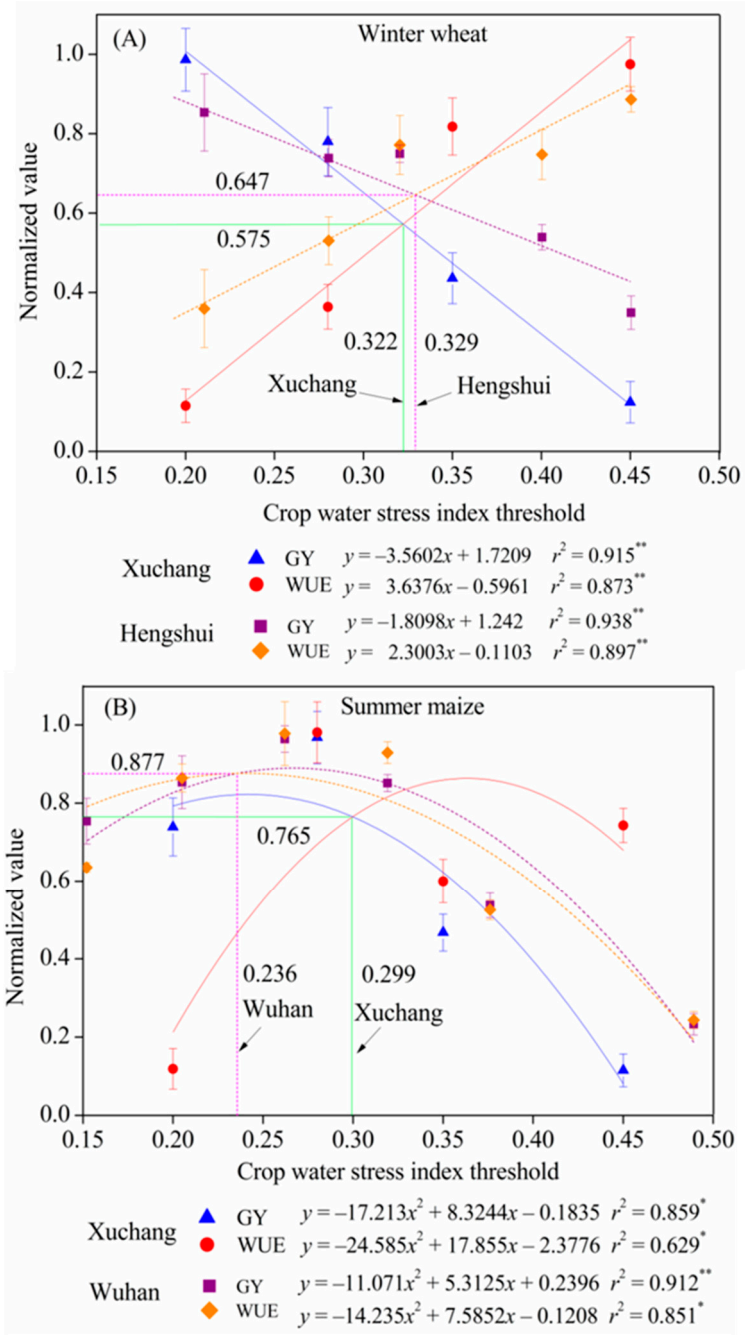

Figure 8. The relationship between grain yield (GY, *y*)/water use efficiency (WUE, *y*) and crop water stress index threshold (CWSI, *x*) for (**A**) winter wheat and (**B**) summer maize based on field experiments conducted at the Xuchang Irrigation Experiment Station in the 2019–2020 growing season. Data from Hengshui [68] and Wuhan [69] were adopted to compare the CWSI thresholds for winter wheat and summer maize from Xuchang. Date were reconstructed and reproduced with the permission from Zhao Y., Master's Degree Dissertation; published by Chinese Academy of Agricultural Sciences, Beijing, China, 2016; and Wang S., Master's Degree Dissertation; published by Huazhong Agricultural University, Wuhan, China, 2008. GY and WUE values were normalized before use. Vertical error bars indicate standard deviation (SD). * and ** mean significant correlation at $p < 0.05$ and $p < 0.01$, respectively. Adapted with permission from Ref. [68]. 2016, Zhao Y. Adapted with permission from Ref. [69]. 2008, Wang S.

In addition, through the linear equations between $T_c - T_a$ (y) and CWSI (x) ($r^2 \geq 0.719$), $T_c - T_a$ threshold can be determined (Table 3). In this study, the thresholds of $T_c - T_a$ were

estimated to 0.925 °C for winter wheat and 0.498 °C for summer maize, respectively. The results confirm the previous conclusion that wheat might be more tolerant to water stress than maize, since it had higher thresholds of $T_c - T_a$ [27,69]. Several studies believed that $T_c - T_a > 0$ °C was the limit value of water shortage for most crops, which was slightly lower than the results from this study [29,57]. The higher thresholds of $T_c - T_a$ were probably attributable to the deficit irrigation regimes with the CPIS in this experiment. We considered that $T_c - T_a > 0.5$ °C for summer maize and $T_c - T_a > 0.9$ °C for winter wheat should be used as a reference index for irrigation decision-making in the NCP. Compared with CWSI, $T_c - T_a$ values are more accessible, making irrigation scheduling much easier than CWSI-based approaches [71–73]. Those thresholds help us obtain higher GY with less water.

Table 3. Using correlation between $T_c - T_a$ (y, °C) and CWSI (x) to determine the $T_c - T_a$ threshold (°C) for winter wheat and summer maize.

Crop	Linear Function	CWSI Threshold	$T_c - T_a$ Threshold	r^2
Wheat	$y = 16.565x - 4.4094$	0.322	0.925	0.719 *
Maize	$y = 16.533x - 4.4458$	0.299	0.498	0.868 *

Note: * means significant correlation at $p < 0.05$.

4. Conclusions

In conclusion, the soil water content was depleted at maturity by winter wheat, causing a noticeably low soil water content during the vegetative period of summer maize. This explained why CWSI thresholds in wheat seasons also exerted an influence on maize plants under rain-fed conditions. The crop water stress index (CWSI) had significant linear relationship with $T_c - T_a$. In this study, we defined the reliable threshold as the one that achieved the dual goal of high GY and high WUE. Based on the definition, we considered that the cross values of the two functions were optimal threshold values that satisfied the goal. In this study, CWSI thresholds were proposed as 0.322 for winter wheat, and 0.299 for summer maize, corresponding to a $T_c - T_a$ threshold value of 0.925 and 0.498 °C, respectively. Compared with traditional soil moisture measurement, the measurement of CWSI and $T_c - T_a$ was a non-destructive, non-contact, and reliable way for the precise estimation of crop water deficit. We conclude that farmers can achieve the dual goal of high GY and high WUE using the optimal thresholds proposed for a winter wheat–summer maize cropping system in the NCP.

Supplementary Materials: The following are available online at https://www.mdpi.com/article/10.3390/agriculture11100958/s1, Table S1. Goodness of fit between soil water content (SWC, % *v/v*) measured using Insentek sensors and oven-dry method across different soil textures in the laboratory at the Xuchang Irrigation Experiment Station in 2017-2018. Figure S1. Seasonal variations in soil water content (SWC, % *v/v*) under (A) I1, (B) I2, (C) I3, and (D) I4 treatments in a winter wheat–summer maize cropping system during the 2019-2020 growing season.

Author Contributions: Conceptualization, A.Q. and D.N.; methodology, Z.L.; software, Z.L.; validation, D.N., Z.L. and B.Z.; formal analysis, A.D.; investigation, A.Q.; resources, A.Q.; data curation, A.D.; writing—original draft preparation, A.Q.; writing—review and editing, D.N.; visualization, D.N.; supervision, A.D.; project administration, A.D.; funding acquisition, S.L. All authors have read and agreed to the published version of the manuscript.

Funding: This research was funded by the China Agriculture Research System (CARS–02), the National Key Research and Development Program (2017YFD0301102), the Central Public-Interest Scientific Institution Basal Research Fund (Farmland Irrigation Research Institute, CAAS, FIRI2020–02), and the Agricultural Science and Technology Innovation Project, CAAS.

Data Availability Statement: The data that support the findings of this study are available from the corresponding authors upon reasonable request.

Acknowledgments: The authors sincerely thank the three anonymous reviewers who made valuable comments on this paper. Many thanks to Zhao Y. and Wang S., who permit the use of some experimental data from their Master's Degree Dissertations. We are also grateful to the staff from the Xuchang Irrigation Experiment Station who provided the technical support for this study.

Conflicts of Interest: The authors declare no conflict of interest. The funders had no role in the design of the study; in the collection, analyses, or interpretation of data; in the writing of the manuscript, or in the decision to publish the results.

References

1. Mekonnen, M.M.; Hoekstra, A.Y. Global Gray Water Footprint and Water Pollution Levels Related to Anthropogenic Nitrogen Loads to Fresh Water. *Environ. Sci. Technol.* **2015**, *49*, 12860–12868. [CrossRef]
2. Campos, N.G.S.; Rocha, A.R.; Gondim, R.; Da Silva, T.L.C.; Gomes, D.G. Smart & Green: An Internet-of-Things Framework for Smart Irrigation. *Sensors* **2019**, *20*, 190. [CrossRef]
3. Qin, A.; Ning, D.; Liu, Z.; Sun, B.; Zhao, B.; Xiao, J.; Duan, A. Structural equation modeling of soil moisture effects on evapo-transpiration of maize in the North China Plain. *Natl. Acad. Sci. Lett.* **2020**, *43*, 219–224. [CrossRef]
4. Li, X.; Zhao, W.; Li, J.; Li, Y. Maximizing water productivity of winter wheat by managing zones of variable rate irrigation at different deficit levels. *Agric. Water Manag.* **2019**, *216*, 153–163. [CrossRef]
5. Qin, A.; Ning, D.; Liu, Z.; Duan, A. Analysis of the Accuracy of an FDR Sensor in Soil Moisture Measurement under Laboratory and Field Conditions. *J. Sens.* **2021**, *2021*, 1–10. [CrossRef]
6. Peng, Y.; Xiao, Y.; Fu, Z.; Dong, Y.; Zheng, Y.; Yan, H.; Li, X. Precision irrigation perspectives on the sustainable water-saving of field crop production in China: Water demand prediction and irrigation scheme optimization. *J. Clean. Prod.* **2019**, *230*, 365–377. [CrossRef]
7. Liu, Z.; Xu, Q. Precision Irrigation Scheduling Using ECH_2O Moisture Sensors for Lettuce Cultivated in a Soilless Substrate Culture. *Water* **2018**, *10*, 549. [CrossRef]
8. Shellie, K.; King, B. Application of a Daily Crop Water Stress Index to Deficit Irrigate *Malbec* Grapevine under Semi-Arid Conditions. *Agriculture* **2020**, *10*, 492. [CrossRef]
9. O'Shaughnessy, S.A.; Evett, S.R.; Colaizzi, P.D. Dynamic prescription maps for site-specific variable rate irrigation of cotton. *Agric. Water Manag.* **2015**, *159*, 123–138. [CrossRef]
10. Time, A.; Acevedo, E. Effects of water deficits on *Prosopis tamarugo* growth, water status and stomata functioning. *Plants* **2021**, *10*, 53. [CrossRef]
11. Egea, G.; Padilla–Díaz, C.M.; Martinez–Guanter, J.; Fernández, J.E.; Perez–Ruiz, M. Assessing a crop water stress index derived from aerial thermal imaging and infrared thermometry in super–high density olive orchards. *Agric. Water Manag.* **2017**, *187*, 210–221. [CrossRef]
12. Ballester-Lurbe, C.; Bello, M.A.J.; Castel, J.; Intrigliolo, D. Usefulness of thermography for plant water stress detection in citrus and persimmon trees. *Agric. For. Meteorol.* **2013**, *168*, 120–129. [CrossRef]
13. Roh, M.; Nam, Y.; Cho, M.; Yu, I.; Choi, G.; Kim, T. Environmental control in greenhouse based on phytomonitoring leaf temperature as a factor controlling greenhouse environments. *Acta Hortic.* **2007**, 71–76. [CrossRef]
14. Shellie, K.C.; King, B.A.; González-Royo, E.; Urtasun, A.; Gil, M.; Kontoudakis, N.; Esteruelas, M.; Fort, F.; Canals, J.M.; Zamora, F. Kaolin Particle Film and Water Deficit Influence Malbec Leaf and Berry Temperature, Pigments, and Photosynthesis. *Am. J. Enol. Vitic.* **2013**, *64*, 223–230. [CrossRef]
15. Bellvert, J.; Zarco-Tejada, P.J.; Girona, J.; Fereres, E. Mapping crop water stress index in a 'Pinot-noir' vineyard: Comparing ground measurements with thermal remote sensing imagery from an unmanned aerial vehicle. *Precis. Agric.* **2013**, *15*, 361–376. [CrossRef]
16. O'Shaughnessy, S.A.; Evett, S.R.; Colaizzi, P.D.; Howell, T.A. Wireless sensor network effectively controls center pivot irriga-tion of sorghum. *Appl. Eng. Agric.* **2013**, *29*, 853–864.
17. Bellvert, J.; Marsal, J.; Girona, J.; Zarco–Tejada, P.J. Seasonal evolution of crop water stress index in grapevine varieties de-termined with high–resolution remote sensing thermal imagery. *Irrig. Sci.* **2015**, *33*, 81–93. [CrossRef]
18. Kacira, M.; Ling, P.P.; Short, T.H. Establishing crop water stress index (CWSI) threshold values for early, non–contact detection of plant water stress. *Trans. ASAE* **2002**, *45*, 775. [CrossRef]
19. Ihuoma, S.O.; Madramootoo, C.A. Recent advances in crop water stress detection. *Comput. Electron. Agric.* **2017**, *141*, 267–275. [CrossRef]
20. Belfiore, N.; Vinti, R.; Lovat, L.; Chitarra, W.; Tomasi, D.; De Bei, R.; Meggio, F.; Gaiotti, F. Infrared Thermography to Estimate Vine Water Status: Optimizing Canopy Measurements and Thermal Indices for the Varieties Merlot and Moscato in Northern Italy. *Agronomy* **2019**, *9*, 821. [CrossRef]
21. Cucho-Padin, G.; Rinza, J.; Ninanya, J.; Loayza, H.; Quiroz, R.; Ramírez, D.A. Development of an Open-Source Thermal Image Processing Software for Improving Irrigation Management in Potato Crops (*Solanum tuberosum* L.). *Sensors* **2020**, *20*, 472. [CrossRef]

22. Gutiérrez–Gordillo, S.; García–Tejero, I.F.; Durán Zuazo, V.H.; García Escalera, A.; Ferrera Gil, F.; Amores–Agüera, J.J.; Cárceles Rodríguez, B.; Hernández–Santana, V. Assessing the water–stress baselines by thermal imaging for irrigation management in almond plantations under water scarcity conditions. *Water* **2020**, *12*, 1298. [CrossRef]
23. Jones, H.G.; Serraj, R.; Loveys, B.R.; Xiong, L.; Wheaton, A.; Price, A.H. Thermal infrared imaging of crop canopies for the remote diagnosis and quantification of plant responses to water stress in the field. *Funct. Plant. Biol.* **2009**, *36*, 978–989. [CrossRef] [PubMed]
24. Erdem, T.; Orta, A.H.; Erdem, Y.; Okursoy, H. Crop water stress index for potato under furrow and drip irrigation systems. *Potato Res.* **2005**, *48*, 49–58. [CrossRef]
25. Wang, F.; Xiao, J.; Ming, B.; Xie, R.; Wang, K.; Hou, P.; Liu, G.; Zhang, G.; Chen, J.; Liu, W.; et al. Grain yields and evapotranspiration dynamics of drip-irrigated maize under high plant density across arid to semi-humid climates. *Agric. Water Manag.* **2021**, *247*, 106726. [CrossRef]
26. Yuan, G.; Luo, Y.; Sun, X.; Tang, D. Winter wheat water stress detection based on canopy surface temperature. *Trans. CSAE* **2002**, *18*, 13–17. (In Chinese with English abstract)
27. Chen, S.; Zhang, X.; Chen, S.; Sun, H.; Pei, D. Variation and interrelationship of winter wheat canopy–air temperature difference, leaf water potential and crop water stress index under different water supply conditions. *J. Triticeae Crops* **2005**, *25*, 38–43. (In Chinese with English abstract)
28. Shi, B.; Liu, Y.; Cai, J. Experimental study on using canopy temperature to guide winter wheat irrigation. *Water Sav. Irrig.* **2008**, *4*, 11–14. (In Chinese with English abstract)
29. Wei, Z.; Xu, D.; Liu, Y.; Cai, J. Diagnosis and experimental study on water deficit of winter wheat based on the variation of canopy–air temperature difference. *J. Hydra. Eng.* **2014**, *45*, 984–990. (In Chinese with English abstract)
30. Cui, X.; Xu, L.; Yuan, G.; Wang, W.; Luo, Y. Crop water stress index model for monitoring summer maize water stress based on canopy surface temperature. *Trans. CSAE* **2005**, *21*, 22–24. (In Chinese with English abstract)
31. Yu, L.; Wang, W.; Cui, X.; Sun, D. Comparisons between the empirical and theoretical models based on canopy temperature for monitoring water stress of summer maize. *J. South China Agric. Uni.* **2007**, *28*, 110–112. (In Chinese with English abstract)
32. Zhou, Y. Effect of water stress on eco–physiology index for wheat and corn in North China Plain. Master's Degree Dissertation, Gansu Agricultural University, Lanzhou, China, 4 June 2011; pp. 16–23. (In Chinese with English abstract)
33. Stegman, E.C. Efficient irrigation timing methods for corn production. *Trans. ASAE* **1986**, *29*, 203–210. [CrossRef]
34. Steele, D.D.; Stegman, E.C.; Gregor, B.L. Field comparison of irrigation scheduling methods for corn. *Trans. ASAE* **1994**, *37*, 1197–1203. [CrossRef]
35. National Standards of China (NSC). *China Soil Classification and Code (GB/T 17296–2009)*; NSC: Beijing, China, 2009.
36. Qin, A.; Ning, D.; Liu, Z.; Sun, B.; Zhao, B.; Xiao, J.; Duan, A. Insentek sensor: An alternative to estimate daily crop evapotranspiration for maize plants. *Water* **2019**, *11*, 25. [CrossRef]
37. Peters, R.T.; Evett, S.R. Automation of a center pivot using the temperature–time–threshold method of irrigation scheduling. *J. Irrig. Drain. Eng.* **2008**, *134*, 286–291. [CrossRef]
38. Osroosh, Y.; Khot, L.R.; Peters, R.T. Economical thermal-RGB imaging system for monitoring agricultural crops. *Comput. Electron. Agric.* **2018**, *147*, 34–43. [CrossRef]
39. O'Shaughnessy, S.A.; Hebel, M.A.; Evett, S.R.; Colaizzi, P.D. Evaluation of a wireless infrared thermometer with a narrow field of view. *Comput. Electron. Agric.* **2011**, *76*, 59–68. [CrossRef]
40. Liu, X.; Yang, S.; Xu, J.; Zhang, J.; Liu, J. Effects of soil heat storage and phase shift correction on energy balance closure of paddy fields. *Atmosfera* **2017**, *30*, 39–52. [CrossRef]
41. Xu, J.; Bai, W.; Li, Y.; Wang, H.; Yang, S.; Wei, Z. Modeling rice development and field water balance using AquaCrop model under drying-wetting cycle condition in eastern China. *Agric. Water Manag.* **2018**, *213*, 289–297. [CrossRef]
42. Qin, A.; Fang, Y.; Ning, D.; Liu, Z.; Zhao, B.; Xiao, J.; Duan, A.; Yong, B. Incorporation of Manure into Ridge and Furrow Planting System Boosts Yields of Maize by Optimizing Soil Moisture and Improving Photosynthesis. *Agronomy* **2019**, *9*, 865. [CrossRef]
43. Ru, C.; Hu, X.; Wang, W.; Ran, H.; Song, T.; Guo, Y. Evaluation of the Crop Water Stress Index as an Indicator for the Diagnosis of Grapevine Water Deficiency in Greenhouses. *Horticulturae* **2020**, *6*, 86. [CrossRef]
44. Irmak, S.; Haman, D.Z.; Bastug, R. Determination of Crop Water Stress Index for Irrigation Timing and Yield Estimation of Corn. *Agron. J.* **2000**, *92*, 1221–1227. [CrossRef]
45. Luan, Y.; Xu, J.; Lv, Y.; Liu, X.; Wang, H.; Liu, S. Improving the performance in crop water deficit diagnosis with canopy temperature spatial distribution information measured by thermal imaging. *Agric. Water Manag.* **2020**, *246*, 106699. [CrossRef]
46. Chai, Q.; Qin, A.; Gan, Y.; Yu, A. Higher yield and lower carbon emission by intercropping maize with rape, pea, and wheat in arid irrigation areas. *Agron. Sustain. Dev.* **2013**, *34*, 535–543. [CrossRef]
47. Radin, J.W.; Mauney, J.R.; Kerridge, P.C. Water Uptake by Cotton Roots during Fruit Filling in Relation to Irrigation Frequency. *Crop. Sci.* **1989**, *29*, 1000–1005. [CrossRef]
48. Wu, X.; Zhang, W.; Liu, W.; Zuo, Q.; Shi, J.; Yan, X.; Zhang, H.; Xue, X.; Wang, L.; Zhang, M.; et al. Root-weighted soil water status for plant water deficit index based irrigation scheduling. *Agric. Water Manag.* **2017**, *189*, 137–147. [CrossRef]
49. Macias–Bobadilla, I.; Vargas–Hernandez, M.; Guevara–Gonzalez, R.G.; Rico–Garcia, E.; Ocampo–Velazquez, R.V.; Torres–Pacheco, I. Differential response to water deficit in chili pepper (*Capsicum annuum* L.) growing in two types of soil under different irrigation regimes. *Agriculture* **2020**, *10*, 381. [CrossRef]

50. Crosby, T.W.; Wang, Y. Effects of irrigation management on chipping potato (*Solanum tuberosum* L.) production in the upper midwest of the U.S. *Agronomy* **2021**, *11*, 768. [CrossRef]
51. Islam, M.A.; De, R.K.; Hossain, M.A.; Haque, M.S.; Uddin, M.N.; Fakir, M.S.A.; Kader, M.A.; Dessoky, E.S.; Attia, A.O.; El–Hallous, E.I.; et al. Evaluation of the tolerance ability of wheat genotypes to drought stress: Dissection through culm–reserves contribution and grain filling physiology. *Agronomy* **2021**, *11*, 1252. [CrossRef]
52. Al-Ghzawi, A.L.A.; Khalaf, Y.B.; Al-Ajlouni, Z.I.; Al-Quraan, N.A.; Musallam, I.; Hani, N.B. The Effect of Supplemental Irrigation on Canopy Temperature Depression, Chlorophyll Content, and Water Use Efficiency in Three Wheat (*Triticum aestivum* L. and *T. durum* Desf.) Varieties Grown in Dry Regions of Jordan. *Agriculture* **2018**, *8*, 67. [CrossRef]
53. Kendall, C.D.; Saleh, T.; Thomas, J.; Trout, C.; Louise, H.; Comas, C. Comparison of canopy temperature–based water stress indices for maize. *Agric. Water Manag.* **2015**, *156*, 51–62.
54. Alordzinu, K.; Li, J.; Lan, Y.; Appiah, S.; AL Aasmi, A.; Wang, H. Rapid Estimation of Crop Water Stress Index on Tomato Growth. *Sensors* **2021**, *21*, 5142. [CrossRef]
55. Antoniuk, V.; Manevski, K.; Kørup, K.; Larsen, R.; Sandholt, I.; Zhang, X.; Andersen, M. Diurnal and Seasonal Mapping of Water Deficit Index and Evapotranspiration by an Unmanned Aerial System: A Case Study for Winter Wheat in Denmark. *Remote Sens.* **2021**, *13*, 2998. [CrossRef]
56. Liang, Z.; Liu, X.; Xiong, J.; Xiao, J. Water Allocation and Integrative Management of Precision Irrigation: A Systematic Review. *Water* **2020**, *12*, 3135. [CrossRef]
57. Sepaskhah, A.; Kashefipour, S. Relationships between leaf water potential, CWSI, yield and fruit quality of sweet lime under drip irrigation. *Agric. Water Manag.* **1994**, *25*, 13–21. [CrossRef]
58. Jones, H.G.; Stoll, M.; Santos, T.; de Sousa, C.; Chaves, M.M.; Grant, O.M. Use of infrared thermography for monitoring stomatal closure in the field: Application to grapevine. *J. Exp. Bot.* **2002**, *53*, 2249–2260. [CrossRef] [PubMed]
59. Payero, J.O.; Irmak, S. Variable upper and lower crop water stress index baselines for corn and soybean. *Irrig. Sci.* **2006**, *25*, 21–32. [CrossRef]
60. Moller, M.; Alchanatis, V.; Cohen, Y.; Meron, M.; Tsipris, J.; Naor, A.; Ostrovsky, V.; Sprintsin, M.; Cohen, S. Use of thermal and visible imagery for estimating crop water status of irrigated grapevine. *J. Exp. Bot.* **2006**, *58*, 827–838. [CrossRef]
61. Shi, J.; Wu, X.; Wang, X.; Zhang, M.; Han, L.; Zhang, W.; Liu, W.; Zuo, Q.; Wu, X.; Zhang, H.; et al. Determining threshold values for root-soil water weighted plant water deficit index based smart irrigation. *Agric. Water Manag.* **2019**, *230*, 105979. [CrossRef]
62. Gonzalez-Dugo, V.; Zarco-Tejada, P.J.; Fereres, E. Applicability and limitations of using the crop water stress index as an indicator of water deficits in citrus orchards. *Agric. For. Meteorol.* **2014**, *198–199*, 94–104. [CrossRef]
63. Niu, Y.; Zhang, H.; Han, W.; Zhang, L.; Chen, H. A Fixed-Threshold Method for Estimating Fractional Vegetation Cover of Maize under Different Levels of Water Stress. *Remote Sens.* **2021**, *13*, 1009. [CrossRef]
64. Ninanya, J.; Ramírez, D.; Rinza, J.; Silva-Díaz, C.; Cervantes, M.; García, J.; Quiroz, R. Canopy Temperature as a Key Physiological Trait to Improve Yield Prediction under Water Restrictions in Potato. *Agronomy* **2021**, *11*, 1436. [CrossRef]
65. Romero-Trigueros, C.; Gambín, J.M.B.; Tortosa, P.A.N.; Cabañero, J.J.A.; Nicolás, E.N. Determination of Crop Water Stress Index by Infrared Thermometry in Grapefruit Trees Irrigated with Saline Reclaimed Water Combined with Deficit Irrigation. *Remote Sens.* **2019**, *11*, 757. [CrossRef]
66. Ballester, C.; Brinkhoff, J.; Quayle, W.C.; Hornbuckle, J. Monitoring the Effects of Water Stress in Cotton using the Green Red Vegetation Index and Red Edge Ratio. *Remote Sens.* **2019**, *11*, 873. [CrossRef]
67. Nemeskéri, E.; Helyes, L. Physiological Responses of Selected Vegetable Crop Species to Water Stress. *Agronomy* **2019**, *9*, 447. [CrossRef]
68. Zhao, Y. Water deficit indicators of winter wheat and their diagnosing thresholds based on response to grain yield. Master's Degree Dissertation, Chinese Academy of Agricultural Sciences, Beijing, China, 25 May 2016; pp. 21–32. (In Chinese with English abstract)
69. Wang, S. Effect of N rates on growth of summer maize and drought threshold under different drought levels. Master's Degree Dissertation, Huazhong Agricultural University, Wuhan, China, 11 June 2008; pp. 16–28, (In Chinese with English abstract).
70. Gontia, N.; Tiwari, K. Development of crop water stress index of wheat crop for scheduling irrigation using infrared thermometry. *Agric. Water Manag.* **2008**, *95*, 1144–1152. [CrossRef]
71. Matese, A.; Baraldi, R.; Berton, A.; Cesaraccio, C.; Di Gennaro, S.F.; Duce, P.; Facini, O.; Mameli, M.G.; Piga, A.; Zaldei, A. Estimation of Water Stress in Grapevines Using Proximal and Remote Sensing Methods. *Remote Sens.* **2018**, *10*, 114. [CrossRef]
72. Matese, A.; Di Gennaro, S.F. Practical Applications of a Multisensor UAV Platform Based on Multispectral, Thermal and RGB High Resolution Images in Precision Viticulture. *Agriculture* **2018**, *8*, 116. [CrossRef]
73. O'Shaughnessy, S.A.; Evett, S.R.; Colaizzi, P.D.; Howell, T.A. A crop water stress index and time threshold for automatic irrigation scheduling of grain sorghum. *Agric. Water Manag.* **2012**, *107*, 122–132. [CrossRef]